Small Platinum−Thallium Clusters Stabilized by Ethylenediamine, $[(NC)_5Pt-Tl(en)_{n-1}]$ ($n = 1-3$) − Characterization in Solution and in the Solid State

Guibin Ma,[a][‡] Mikael Kritikos,[b] and Julius Glaser*[a]

Keywords: Metal−metal interactions / Platinum / Thallium / N ligands / NMR spectroscopy

Three neutral binuclear platinum–thallium compounds containing a direct and "naked" (unsupported by ligands) metal–metal bond have been prepared in dimethyl sulfoxide (DMSO). The compounds have the formula $[(NC)_5Pt–Tl(en)_{n-1}]$ (n = 1–3, for compounds **1**, **2** and **3**, respectively) and were found to exist in solution by means of multinuclear NMR (^{195}Pt, ^{205}Tl, ^{13}C and ^{1}H) and Raman spectroscopy. The compounds exhibit very large single bond $^{195}Pt–^{205}Tl$ spin-spin coupling constants of 48–66 kHz. In addition, the solid state analogues of **1** and **3**, $[(NC)_5Pt–Tl(DMSO)_4](DMSO)$ and $[(NC)_5Pt–Tl(en)_2](DMSO)_2$, were synthesized and their structures determined by single crystal X-ray diffraction. The metal–metal bond lengths of Pt–Tl are 2.6131(4) Å and 2.6348(5) Å in compounds **1** and **3**, respectively. Crystal data for compound **1:** monoclinic, space group *Cc* (No. 9), $Z = 4$, $a = 17.2367(14)$, $b = 9.5560(11)$, $c = 17.7941(15)$ Å, $\beta = 100.551(10)°$, $V = 2881.4(5)$ Å^3, $T = 110(1)$ K; and for compound **3:** monoclinic, space group $P2_1$ (No. 4), $Z = 2$, $a = 9.3167(14)$, $b = 12.3007(13)$, $c = 11.4586(16)$ Å, $\beta = 112.318(16)°$, $V = 1214.8(3)$ Å^3, $T = 110(1)$ K.

Introduction

A direct metal−metal bond between platinum and thallium atoms in the solid state was first described by Nagle et al.[1] Later, the binuclear compound $[Pt(CN)_2Tl(crown\text{-}P_2)](NO_3)$ {Crown-P_2: 1,10-bis[(diphenylphosphanyl)methyl]-1,10-diaza-4,7,13,16-tetraoxaoctadecane, formula: $C_{38}H_{48}N_2O_4P_2$}[2] and trinuclear Pt−Tl−Pt compounds, e.g. *cis*-$[Tl\{(1\text{-methylthyminato})_2Pt(NH_3)_2\}_2](NO_3)\cdot 7H_2O$[3] and $(NBu_4)_2[Tl\{Pt(C_6F_5)_4\}_2]$,[4] with Pt−Tl metal−metal bonds, have been synthesized. Three compounds containing a slightly larger Pt−Tl cluster unit have also been prepared, namely $[TlPt_3(CO)_3(PCy_3)_3][Rh(\eta\text{-}C_8H_{12})Cl_2]$ (Cy = cyclohexyl),[5] $[TlPt_6(\mu\text{-}CO)_6(\mu\text{-}dppp)_3]^+$ [dppp = $(C_6H_5)_2P(CH_2)_3P(C_6H_5)_2$],[6] and $[Pt_3\{\mu_3\text{-}Tl(acac)\}(ReO_3)(\mu\text{-}dppm)_3]^+$ [dppm = $(C_6H_5)_2PCH_2P(C_6H_5)_2$].[7] Hao et al.[8] have prepared hexaplatinum clusters with carbonyl and diphosphane ligands, e.g. $[Pt_6(\mu\text{-}CO)_6(\mu\text{-}dppp)_2(dppp)_2]$, and were able to trap Hg^0 and Tl^I in $[Pt_6(\mu_6\text{-}Hg)(\mu\text{-}CO)_6(\mu\text{-}dppp)_3]$ and $[Pt_6(\mu_6\text{-}Tl)(\mu\text{-}CO)_6(\mu\text{-}dppp)_3]^+$, respectively. In the latter compound, the Pt−Tl bond lengths are in the range of 2.860(3)−2.992(3) Å.

Recently, a new family of four binuclear platinum-thallium cyano compounds with the formula $[(NC)_5Pt-Tl(CN)_{n-1}]^{(1-n)}$ ($n = 1-4$ for compounds **I**, **II**, **III** and **IV,** respectively), which contain a direct metal−metal bond unsupported by the ligands, have been synthesized from $Tl(ClO_4)_3$, $K_2Pt(CN)_4$ and NaCN in aqueous solution.[9−11] The compounds possess long-term stability but undergo photochemically induced two-electron transfer between the metal ions when exposed to daylight. Thus, possible applications in photovoltaic devices, for example in a "wet" solar cell of the Grätzel type[12] can be envisaged. However, several chemico-physical parameters of the compounds, such as stability, electrochemical properties or light absorption characteristics, have to be tuned in order to fit the demands of the cell. Therefore, we have initiated a study of possible modifications of these compounds, including both preparative efforts and experimental and theoretical characterization in solution and in the solid state.

The binuclear compounds **I**−**IV** can be viewed as consisting of two units, $Pt(CN)_5$ and $Tl(CN)_n$. The platinum unit is stable and relatively inert in all four compounds whereas the geometry of the thallium entity changes depending on the number of cyanide ligands;[9,10] these cyanide ligands have been found to be kinetically labile. Hence, there is a possibility to replace the cyanides by other ligands, for example amines or organic solvent molecules. Here, the bidentate ethylenediamine ligand was deemed suitable for further study due to its "robustness" and to the fact that Tl^{III} can form strong complexes with N-donor ligands.[13−15] Recently, it was found in this laboratory that, although Tl^{III} ethylenediamine complexes are difficult to

[a] Department of Chemistry, The Royal Institute of Technology (KTH),
100 44 Stockholm, Sweden
E-mail: julius@inorg.kth.se
[b] Department of Structural Chemistry, Arrhenius Laboratory, Stockholm University,
106 91 Stockholm, Sweden
[‡] Permanent address: Department of Chemistry,
Shanxi University,
030006, Taiyuan, Shanxi Province, P. R. China
Supporting information for this article is available on the WWW under http://www.wiley-vch.de/home/eurjic or from the author.

 © WILEY-VCH Verlag GmbH, 69451 Weinheim, 2001 1434−1948/01/0505−1311 $ 17.50+.50/0

prepare in aqueous solution, very stable complexes are formed in organic solvents.[16]

In the present paper, complexes of $[(NC)_5Pt-Tl(en)_{n-1}]$ ($n = 1-3$) with a direct Pt−Tl bond have been studied both in DMSO solution and in the solid state.

Results and Discussion

Characterization in Solution by Multinuclear NMR Spectroscopy

The binuclear complexes $[(NC)_5Pt-Tl(DMSO)_4]$ (**1**), $[(NC)_5Pt-Tl(en)(DMSO)_x]$ (**2**) and $[(NC)_5Pt-Tl(en)_2]$ (**3**) were prepared in DMSO solvent according to the following reactions:

$$[Tl(dmso)_6]^{3+} + [Pt(CN)_4]^{2-} + CN^- \rightleftharpoons \underset{\mathbf{1}}{[(NC)_5Pt{-}Tl(dmso)_4]} + 2\ DMSO \quad (1)$$

$$[Tl(dmso)_6]^{3+} + en \rightleftharpoons [Tl(en)(dmso)_x]^{3+} + (6{-}x)\ DMSO \quad (2)$$

$$[Tl(en)(dmso)_x]^{3+} + [Pt(CN)_4]^{2-} + CN^- \rightleftharpoons \underset{\mathbf{2}}{[(NC)_5Pt{-}Tl(en)(dmso)_x]} \quad (3)$$

$$[Tl(en)_3]^{3+} + [Pt(CN)_4]^{2-} + CN^- \rightleftharpoons \underset{\mathbf{3}}{[(NC)_5Pt{-}Tl(en)_2]} + en \quad (4)$$

The compounds **1**, **2** and **3** were prepared, according to the reactions in Equation (1) to (4), in solutions in which the composition was varied in order to achieve different en/Pt−Tl ratios. The content and the concentration of the compounds in each solution were determined by means of ^{205}Tl and ^{195}Pt NMR spectroscopy. Since the chemical shifts of the three compounds fall in different regions (see Table 1), and the spin−spin coupling patterns represent "fingerprints" of each compound, the composition of the solutions could be easily determined.

$[(NC)_5Pt-Tl(en)_2]$ (3)

Reaction of $[Tl(en)_3](ClO_4)_3$, $K_2Pt(CN)_4$ and NaCN [Equation (4)] in DMSO yielded a colorless solution. The ^{195}Pt and ^{205}Tl NMR spectra of this solution showed the existence of only one Pt−Tl bonded complex (Figure 1 a, b). The ^{205}Tl NMR spectrum (Figure 1a) of the resulting solution shows one triplet signal (with the intensity ratio 1:3.9:1) centered at $\delta = 1885$. Two small symmetrical peaks at both sides (with a very large spin-spin coupling constant, ≈48 kHz) arise from spin-spin coupling between the ^{205}Tl and ^{195}Pt nuclei (^{195}Pt: $I = 1/2$, natural abundance 33.8%); together with the central uncoupled peak they give the intensity ratio of 1:3.9:1 as expected for one thallium coupled to one platinum atom. Another peak at $\delta = 2900$ was detected in the ^{205}Tl NMR spectrum of this solution and was assigned to the unreacted $[Tl(en)_3]^{3+}$ complex. The ^{195}Pt NMR spectrum of the Pt−Tl compound (Figure 1b) consists of a 1:1 doublet centered at $\delta = 370$ due to the coupling between ^{195}Pt and ^{205}Tl (^{205}Tl: $I = 1/2$, natural abundance 70.5%) with the same Pt−Tl coupling constant ≈48 kHz to ^{205}Tl as observed in the ^{205}Tl NMR spectrum. In addition, there is another barely resolved doublet due to the coupling of ^{195}Pt to the other thallium isotope, ^{203}Tl, with $I = 1/2$ and natural abundance 29.5%. The huge spin-spin coupling constant of $^1J(^{205}Tl-^{195}Pt)$ ≈48 kHz indicates formation of a direct Pt−Tl bond.

A ^{13}C NMR spectrum of the 99% ^{13}CN enriched complex showed that two types of coordinated cyanides exist in $[(NC^{13})_5Pt-Tl(en)_2]$ (Figure 2). One signal appears at $\delta = 97.3$ with spin-spin coupling constants $^2J(^{13}C^A-^{205}Tl) = 9150$ Hz and $^1J(^{13}C^A-^{195}Pt) = 834$ Hz and is assigned to the axial cyanide, labeled as CN^A. The other signal, at $\delta = 85.9$, with spin-spin coupling constants $^2J(^{13}C^C-^{205}Tl) = 391$ Hz and $^1J(^{13}C^C-^{195}Pt) = 818$ Hz, belongs to the cyanides (CN^C) in the square-planar $Pt(CN)_4$ unit. The ^{13}C NMR signal of the coordinated ethylenediamine ligand overlaps with the signal of deuterated $[D_6]$DMSO at $\delta = 39$. Considering the composition of the solution and the available information on the previously described Pt−Tl complexes **I**−**IV**,[9,10] these findings indicate that the composition of the complex is $[(NC)_5Pt-Tl(en)_2]$.

Table 1. Selected NMR parameters for the complexes $[(NC)_5Pt-Tl(en)_{n-1}]$ ($n = 1-3$) and for some related dimeric (Pt−Tl) and monomeric platinum and thallium species in solution; for the notation of the carbon/cyanide sites in the platinum-thallium cyano complexes, see Figure 6;

	δ_{Tl} [a]	δ_{Pt} [a]	$\delta_C{}^A$	$\delta_C{}^C$	$^1J_{Pt-Tl}$ (Hz)	$^2J_{Tl-C}{}^A$ (Hz)	$^2J_{Tl-C}{}^C$ (Hz)	$^1J_{Pt-C}{}^A$ (Hz)	$^1J_{Pt-C}{}^C$ (Hz)
Tl^{I}[b]	361								
$[Pt^{IV}(CN)_6]^{2-}$[c]		655		100.7					876
$[Tl^{III}(DMSO)_6]^{3+}$ [b]	1889								
$[Tl(en)_3]^{3+}$ in DMSO[b]	2900								
$[(NC)_5Pt-Tl(DMSO)_x]$[b]	887	574	84.7	83.9	65854	12213	605	920	811
$[(NC)_5Pt-Tl(en)(DMSO)_x]$[b]	1448	494	91.3	84.2	55100	9911	480	880	816
$[(NC)_5Pt-Tl(en)_2]$[b]	1885	370	97.3	85.9	47850	9150	391	834	818
$[(NC)_5Pt-Tl]$[c]	786	474	93.4	90.3	71060	12746	592	909	820
$[(NC)_5Pt-Tl(CN)_3]^{3-}$ [c]	2224	68	116.1	97.0	38760	7270	255	742	843
$[Tl^{III}(CN)_2]^+$ [c]	2447								
$[Pt^{II}(CN)_4]^{2-}$ [b]		−189		121.6					1015
$[Pt^{II}(CN)_4]^{2-}$ [c]		−213		130.2					1031

[a] The ^{205}Tl NMR chemical shift is given in ppm toward higher frequency with respect to an aqueous solution of $TlClO_4$ extrapolated to infinite dilution at 25 °C; the ^{195}Pt NMR chemical shift is given in ppm toward higher frequency from $\chi(^{195}Pt) = 21.4$ MHz; $\delta[PtCl_6]^{2-} = 4533$ at 25 °C in aqueous solution. − [b] DMSO solution. − [c] Aqueous solution, ref.[9,10].

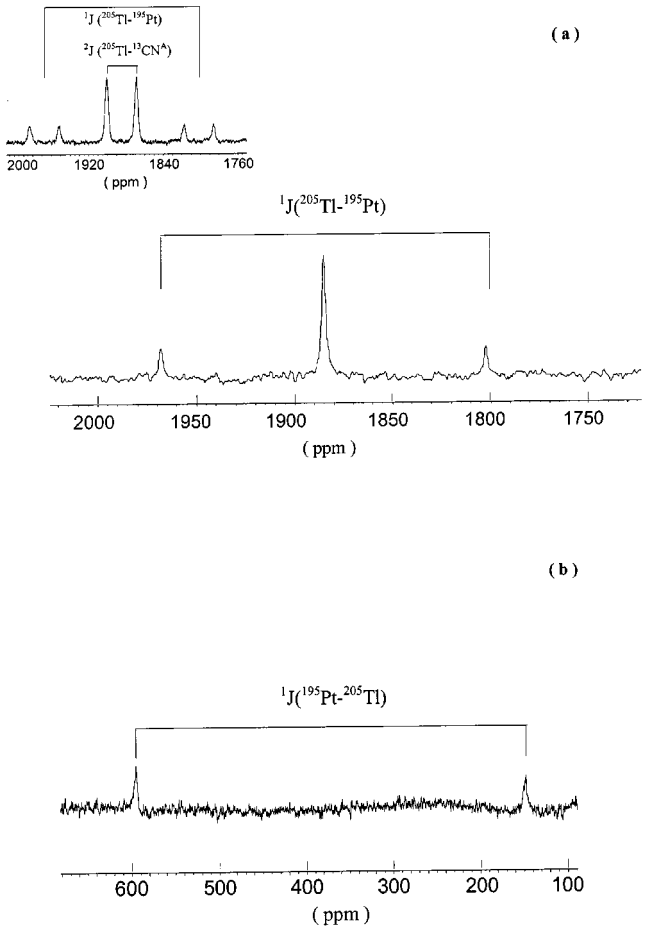

Figure 1. (a) 288.5 MHz ^{205}Tl NMR spectrum of $[(NC)_5Pt-Tl(en)_2]$ in DMSO; the concentrations of $[Tl(en)_3](ClO_4)_3$, $K_2Pt(CN)_4$ and NaCN are all 50 mmol/L (the inset shows the spectrum for a solution of the same compound with all cyanide enriched in ^{13}C, 99%); (b) 107.5 MHz ^{195}Pt NMR spectrum of $[(NC)_5Pt-Tl(en)_2]$ in the same solution, 298 K

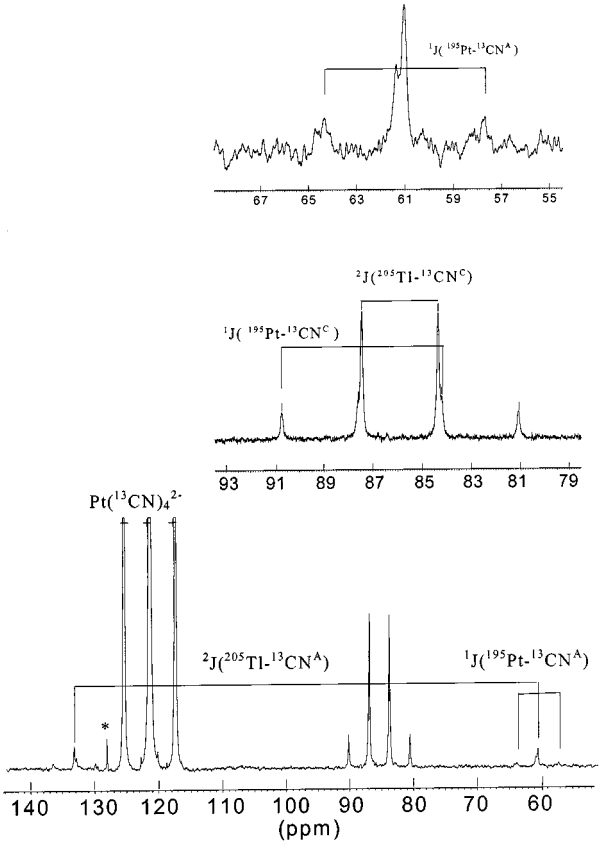

Figure 2. 125.7 MHz ^{13}C NMR of $[(NC^{13})_5Pt-Tl(en)_2]$ in $[D_6]$DMSO solution, 298 K; the composition of the solution is 50 mmol/L $[Tl(en)_3](ClO_4)_3$, 50 mmol/L $NaPt(^{13}CN)_4$ and 50 mmol/L $Na^{13}CN$ (the ^{13}C signal of en at δ = 39 — not shown in the spectrum — overlaps with the ^{13}C signals of the deuterated $[D_6]$DMSO solvent); * impurity; + signals of unreacted $[Pt(^{13}CN)_4]^{2-}$

$[(NC)_5Pt-Tl(DMSO)_4]$ (1) and $[(NC)_5Pt-Tl(en)(DMSO)_x]$ (2)

In a similar way, the two remaining compounds were characterized. The ^{205}Tl NMR spectrum of compound **2** in DMSO solution is a triplet centered at δ = 1448 with the spin-spin coupling constant between ^{205}Tl and ^{195}Pt equal to ≈55 kHz. The ^{195}Pt NMR spectrum of this species is a 1:1 doublet centered at δ = 494 with the same spin-spin coupling constant of about 55 kHz.

For compound **1** in DMSO, the ^{205}Tl NMR chemical shift is δ = 887 and the ^{195}Pt NMR shift is δ = 574 with $^1J(^{205}Tl-^{195}Pt)$ = 65.8 kHz. Selected ^{205}Tl, ^{195}Pt and ^{13}C NMR spectroscopic data of the three compounds are listed in Table 1. (^{205}Tl and ^{195}Pt NMR spectra for compounds **1** and **2** are shown in the Supporting Information).

In the ^{1}H NMR spectra, the signal of the free ethylenediamine CH_2 groups appears at δ = 2.82. For compounds **2** and **3**, signals appear at δ = 3.47 and 3.65, respectively, and are assigned to the protons of the coordinated ethylenediamine ligand.

No metal−metal bonded species were detected when only $[Pt(CN)_4]^{2-}$ and $[Tl(en)_3]^{3+}$ were present in solution. However, with additional cyanide Pt−Tl compounds are formed. This is proved by NMR spectrosocopy (for **1**, **2** and **3)** and X-ray diffraction analysis (for **1** and **3**). Thus, it is apparent that the extra cyanide is necessary for the formation of the Pt−Tl bond.

An important experimental observation should be mentioned in this context: the spin-spin coupling constant $^2J(^{205}Tl-^{13}C)$ for the linear entity ^{A}NC−Pt−Tl (axial cyanide) is more than one order of magnitude larger than that of ^{C}NC−Pt−Tl (equatorial cyanides, i.e. C−N^C is perpendicular to the Pt−Tl bond), cf. Table 1. This indicates that the fifth cyano ligand plays a key role in stabilization of the Pt−Tl bond. It can be explained by an overlap of the Tl s orbital, the Pt d_z^2 orbital and the CN p_z orbital to form a molecular orbital ^{A}NC−Pt−Tl along the *z* axis: thus, the linear ^{A}NC−Pt−Tl- unit is stabilized.

Raman Spectra of 1 and 3 in the Solid State

A characteristic feature of the Raman spectra of the Pt−Tl compounds in aqueous solution is the presence of a strong and sharp band in the low frequency region,[10] which is due to the metal−metal (M−M) bond stretch-

ing.[17] In general, bimetallic compounds with unsupported single metal−metal bonds display M−M stretching bands at wave numbers lower than 200 cm^{-1}, while multiple bonding or ligand bridging in conjunction with an M−M single bond leads to higher wavenumbers.[18] The Raman spectra of the solid compounds **1** and **3** exhibit metal−metal vibrations at 154 cm^{-1} and 156 cm^{-1}, respectively.

The C≡N stretching region of the binuclear species is also informative and can provide an additional support for the structure of the compounds. We assign the two sharp bands at 2174 cm^{-1}, 2161 cm^{-1} for **1** and at 2168 cm^{-1}, 2151 cm^{-1} for **3** to the symmetric (A_{1g}) and antisymmetric (B_{1g}) stretching vibrations of the four equivalent cyanides ($C{\equiv}N^C$) of the $Pt(CN)_4$ unit in D_{4h} symmetry[19] in the compounds $[(^CNC)_4(^ANC)Pt-Tl(en)_{n-1}]$ ($n = 1-3$). These bands shift to high frequency and are very close to the stretching bands at 2153 cm^{-1}(s) and 2137 cm^{-1}(m) for the $[Pt(CN)_4]^{2-}$ complex in the solid state. The higher frequency bands at 2184 cm^{-1} and 2179 cm^{-1} are assigned to the $C{\equiv}N^A$ ligand in compounds **1** and **3**, respectively.

Crystal Structures of $[(NC)_5Pt-Tl(DMSO)_4](DMSO)$ (1) and $[(NC)_5Pt-Tl{\cdot}(en)_2](DMSO)_2$ (3)

The structures of **1** and **3** in the solid state were determined by single crystal X-ray crystallography and are shown in Figure 3 and 4, respectively. Selected bond lengths and angles of **1** and **3** are given in Table 2 and 3, respectively.

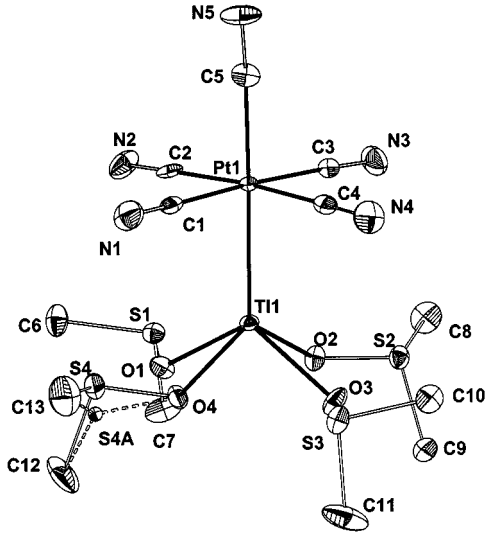

Figure 3. ORTEP view of the binuclear complex $[(NC)_5Pt-Tl(DMSO)_4]$ in the crystal structure of $[(NC)_5Pt-Tl(DMSO)_4](DMSO)$ (ellipsoids at 50% probability level)

In the structure of **1**, a $Pt(CN)_5$ unit is bonded to a $Tl(DMSO)_4$ unit with a Pt−Tl bond length of 2.6131(4) Å. The difference in bond length between the axial and equatorial cyanide groups is less pronounced than in complex **3**. In **1**, the equatorial Pt−C bond lengths are around 2.01(1) Å while the axial Pt−C bond length is 2.037(7) Å. Four crystallographically different DMSO groups are coordinated to thallium with Tl−O bond lengths in the range 2.287(5) to 2.311(4) Å. The Tl atom is coordinated in a square pyramidal fashion, and is located 1.08 (1) Å from the basal plane defined by the four O atoms. In the same way as in **3** (see below), the two en groups and the four cyano ligands are arranged in an eclipsed geometry.

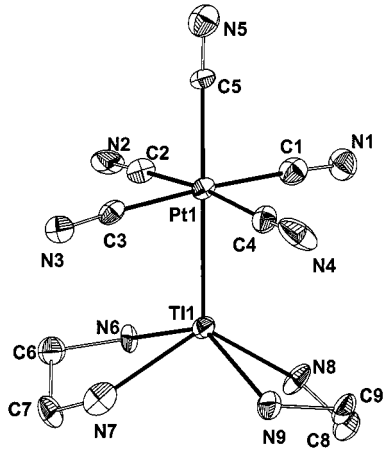

Figure 4. ORTEP view of the binuclear complex $[(NC)_5Pt-Tl(en)_2]$ in the crystal structure of $[(NC)_5Pt-Tl(en)_2](DMSO)_2$ (ellipsoids at 50% probability level)

Table 2. Selected bond lengths (Å) and angles (°) in the crystal structure of $[(NC)_5Pt-Tl(DMSO)_4]{\cdot}(DMSO)$ (**1**)

Tl1−Pt1	2.6131(4)	S1−O1	1.543(6)
Tl1−O1	2.292(5)	S2−O2	1.540(4)
Tl1−O2	2.290(5)	S3−O3	1.543(6)
Tl1−O3	2.287(5)	S4−O4	1.533(5)
Tl1−O4	2.311(4)	S5−O5	1.500(8)
Pt1−C1	2.008(7)	S1−C6	1.779(7)
Pt1−C2	2.018(7)	S1−C7	1.778(9)
Pt1−C3	2.017(8)	S2−C8	1.774(9)
Pt1−C4	2.009(7)	S2−C9	1.768(9)
Pt1−C5	2.037(7)	S3−C10	1.768(7)
N1−C1	1.148(10)	S3−C11	1.779(11)
N2−C2	1.147(10)	S4−C12	1.797(11)
N3−C3	1.147(10)	S4−C13	1.776(12)
N4−C4	1.144(10)	S5−C14	1.760(10)
N5−C5	1.148(10)	S5−C15	1.808(5)
Pt1−C1−N1	177.1(7)	Pt1−Tl1−O3	120.68(1)
Pt1−C2−N2	178.8(6)	Pt1−Tl1−O4	113.97(1)
Pt1−C3−N3	178.5(7)	O1−Tl1−O2	76.30(16)
Pt1−C4−N4	179.4(7)	O1−Tl1−O3	119.73(1)
Pt1−C5−N5	175.5(6)	O1−Tl1−O4	76.93(17)
C1−Pt1−C3	176.8(3)	O2−Tl1−O3	76.29(18)
C1−Pt1−C4	89.1(3)	O2−Tl1−O4	127.24(1)
C1−Pt1−C5	89.2(3)	O3−Tl1−O4	78.96(17)
C1−Pt1−C2	89.3(3)	Tl1−Pt1−C1	89.7(2)
C2−Pt1−C3	92.3(3)	Tl1−Pt1−C2	86.7(2)
C2−Pt1−C4	175.7(3)	Tl1−Pt1−C3	87.6(2)
C2−Pt1−C5	92.3(3)	Tl1−Pt1−C4	89.3(2)
C3−Pt1−C4	89.2(3)	Tl1−Pt1−C5	178.5(2)
C3−Pt1−C5	93.6(3)	Tl1−O1−S1	120.1(2)
C4−Pt1−C5	91.6(3)	Tl1−O2−S2	119.5(3)
Pt1−Tl1−O1	119.58(1)	Tl1−O3−S3	121.8(3)
Pt1−Tl1−O2	118.76(1)	Tl1−O4−S4	115.1(3)

The structure of **3** is closely related to that of **1**. The $Pt(CN)_5$ unit is bonded to the $Tl(en)_2$ group with a Pt−Tl bond length of 2.6348(5) Å. The coordination around Pt consists of two kinds of cyanide groups. The axial cyanide has a Pt−C bond length of 2.082(6) Å, whereas the four cyanide groups located in a square around the metal ion have considerably shorter Pt−C bond lengths of 2.01(1) Å.

Table 3. Selected bond lengths [Å] and angles [°] in the crystal structure of $[(NC)_5Pt-Tl(en)_2](DMSO)_2$ (**3**)

Tl1−Pt1	2.6348(5)	N1−C1	1.140(8)
Tl1−N6	2.376(8)	N2−C2	1.142(8)
Tl1−N7	2.394(10)	N3−C3	1.139(8)
Tl1−N8	2.361(14)	N4−C4	1.142(8)
Tl1−N9	2.373(17)	N5−C5	1.134(7)
Pt1−C1	2.012(7)	N6−C6	1.494(18)
Pt1−C2	2.015(7)	N7−C7	1.50(2)
Pt1−C3	2.007(7)	N8−C8	1.470(10)
Pt1−C4	2.012(7)	N9−C9	1.466(10)
Pt1−C5	2.082(6)	C6−C7	1.497(15)
		C8−C9	1.485(15)
Pt1−Tl1−N6	108.3(3)	C1−Pt1−C2	89.4(6)
Pt1−Tl1−N7	115.2(4)	C1−Pt1−C3	175.4(6)
Pt1−Tl1−N8	123.4(3)	C1−Pt1−C4	91.4(6)
Pt1−Tl1−N9	113.2(3)	C1−Pt1−C5	91.7(9)
Tl1−N6−C6	107.6(9)	C2−Pt1−C3	88.3(6)
Tl1−N7−C7	108.8(9)	C2−Pt1−C4	173.0(6)
Tl1−N8−C8	111.9(9)	C2−Pt1−C5	94.9(8)
Tl1−N9−C9	105.7(9)	C3−Pt1−C4	90.5(6)
N6−Tl1−N7	75.2(5)	C3−Pt1−C5	92.4(9)
N6−Tl1−N8	85.7(5)	C4−Pt1−C5	92.0(8)
N6−Tl1−N9	138.3(5)	Tl1−Pt1−C1	88.9(5)
N7−Tl1−N8	121.4(5)	Tl1−Pt1−C2	85.4(5)
N7−Tl1−N9	84.1(5)	Tl1−Pt1−C3	87.0(5)
N8−Tl1−N9	74.8(5)	Tl1−Pt1−C4	87.6(4)
Pt1−C1−N1	176.1(14)	Tl1−Pt1−C5	179.3(9)
Pt1−C2−N2	177.1(15)	N6−C6−C7	108.9(11)
Pt1−C3−N3	176.8(15)	N7−C7−C6	114.3(10)
Pt1−C4−N4	176.6(14)	N8−C8−C9	113.2(10)
Pt1−C5−N5	176(3)	N9−C9−C8	113.7(11)

Thallium has a distorted square pyramidal coordination geometry and is located 1.00 (1) Å from the basal plane defined by the four N atoms. The two en ligands and the four cyanide groups form an eclipsed conformation to each other.

The Pt−Tl bond lengths in compounds **1** and **3** are significantly shorter than the Pt−Tl bond lengths in $[Tl(crown\text{-}P_2)Pt(CN)_2]^+$ [2.911(2) and 2.958(2) Å] [2] and in $[Pt_6(\mu_6\text{-}Tl)(\mu\text{-}CO)_6(\mu\text{-}dppp)_3]^+$ [2.860(3) − 2.992(3) Å],[8] in which the oxidation states of the metal ions are Pt^{2+} and Tl^+, but very similar to the Pt−Tl bond lengths in $[(NC)_5Pt-Tl(bipy)(DMSO)_3]$ [2.6187(7) Å] and $[(NC)_5Pt-Tl(bipy)_2]$ [2.6117(5) Å] in which the sum of the oxidation states is +5.[20] In the Pt−Tl cyano complexes, $[(NC)_5Pt-Tl(CN)_{n-1}]^{(1-n)}$ (n = 2−4), studied in aqueous solution by the EXAFS technique,[21] the Pt−Tl bond lengths are in the range 2.598−2.638 Å. The Pt−Tl bond length increases with increasing number of cyano ligands attached to the thallium. The X-ray diffraction data show that the Pt−Tl bond lengths in compounds **1** and **3** in the solid state are of the same order of magnitude as those in the Pt−Tl cyano complexes in solution. The Tl−N bond lengths (average 2.376 Å) in **3** are very close to those in $[Tl(en)_3](ClO_4)_3$ (average 2.370 Å),[16] where thallium is hexacoordinated by three en ligands, which is probably due to the lower actual charge on thallium in $[(NC)_5Pt-Tl(en)_2]$ than in $[Tl(en)_3](ClO_4)_3$. The $Tl-O_n$ (n = 1−4) bond lengths in compound **1** (2.287−2.311 Å) are shorter than the Tl−O bond lengths in $[Tl(bipy)_3(DMSO)](ClO_4)_3$ [2.333(10) Å] [20] and in $[TlCl_5(DMSO)]^{2-}$ [2.42(2) Å],[22] but are longer than the Tl−O bond length in $[Tl(DMSO)_6]^{3+}$ [2.224(3) Å].[23]

Discussion

Chemical Shifts

The ^{205}Tl NMR chemical shifts of Tl^{III} complexes are very sensitive to a change in the coordination sphere of the metal ion. In the series of Pt−Tl-en complexes, a linear dependence between δ_{Tl}/δ_{Pt} and the number of coordinated en ligands is observed (Figure 5). A similar behavior was also observed for Tl^{III} ethylenediamine complexes $[Tl(en)_n]^{3+}$ (n = 0−3),[16] where the individual chemical shifts, δ_{Tl}, for the different species were linearly shifted to higher frequency upon an increase of the coordination number.

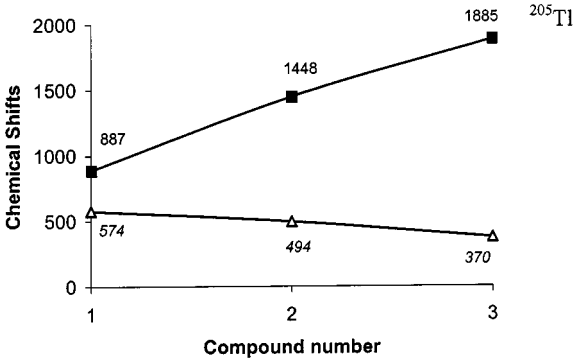

Figure 5. ^{195}Pt and ^{205}Tl NMR chemical shifts for the compounds **1, 2, 3** $[(NC)_5Pt-Tl(en)_{n-1}]$ (n = 1-3, respectively) in DMSO, 298 K; ■ ^{205}Tl NMR; Δ ^{195}Pt NMR

Several earlier studies of Cd^{2+} complexes, which similarly to Tl^{3+} has a d^{10} configuration, indicate the direction and the magnitude of the expected chemical shift change for the complex formation with different ligands, e.g. N-donors to high frequency, O-donors to low frequency.[24−28] A linear correlation between the ^{113}Cd NMR chemical shift and the number of coordinated ligands, very similar to the results of the present work, has also been observed for the Cd-glycine complexes $[Cd(Gly)_n]^{2-n}$ (n = 0−3).[29]

NMR chemical shifts are due to nuclear shielding, which includes the diamagnetic and paramagnetic terms of the Ramsey equation.[30] A theoretical study of metal NMR chemical shifts in metal ion complexes by the ab initio finite perturbation SCF method showed that the paramagnetic term is 10−100 times larger than the diamagnetic contribution.[31] Closed p and d subshells give no contribution to the paramagnetic term, which is caused by the donation of the electrons from the ligands to the metal's outer p orbitals and by the back-donation of electrons from the metal d orbitals to the ligands. Highly electronegative ligands withdraw more σ electrons from the fully occupied d_σ orbitals of the metal. This σ interaction produces holes in the (n − 1)d shell of the metal.[31]

This theoretical description can be used to explain the experimental results observed here for the Tl^{III} complexes.

The coordinated nitrogen (NH_2) is highly electronegative and attracts electrons from Tl d_σ orbitals. The electron cloud density of the thallium atom in its *N*-bonded complexes is lower than without ligands: the higher the ligand coordination number, the lower the electron cloud density around the thallium ion. This effect leads to a deshielding of the thallium nucleus; thus, its chemical shift increases. A similar trend between ^{205}Tl NMR chemical shift and the coordination number was observed in Tl^{III}-cyano complexes, $[Tl(CN)_n]^{3-n}$.[32a]

The ^{195}Pt NMR chemical shift decreases with an increasing number of the Tl-coordinated ethylenediamine ligands in the compounds $[(NC)_5Pt-Tl(en)_{n-1}]$ (n = 1−3). This trend has also been observed in the compounds $[(NC)_5Pt-Tl(CN)_{n-1}]^{(1-n)}$ (n = 1−4)[10] and in $[(NC)_5Pt-Tl(bipy)_{n-1}]$ (n = 2−3).[20] Also for the ^{195}Pt NMR chemical shifts a linear correlation to the number of coordinated ethylenediamine ligands was observed (see Figure 5).

Usually, NMR chemical shifts for heavy metal ions exhibiting a very large chemical shift range are very sensitive to the oxidation state of the metal.[32b,32c] ^{205}Tl NMR chemical shifts of Tl^{I} species are normally in the range from δ = −200 to 200 and those of Tl^{III} species are usually between δ = 2000 and 3000. The ^{195}Pt NMR chemical shifts of $[Pt^{IV}(CN)_6]^{2-}$ and $[Pt^{II}(CN)_4]^{2-}$ are δ = 655 and −213, respectively.[10] In the currently studied compounds, $[(NC)_5Pt-Tl(en)_{n-1}]$ (n = 1−3), the ^{205}Tl NMR chemical shifts fall in the region between Tl^{I} and Tl^{III}, and ^{195}Pt NMR chemical shifts between Pt^{II} and Pt^{IV} (see Table 1). Consequently, the oxidation states of the metal ions in these compounds are close to Pt^{III} and Tl^{II}: this implies that the transfer of two electrons from the substrate $[Pt^{II}(CN)_4]^{2-}$ to Tl^{III} has been partially accomplished. The studied Pt−Tl complexes can thus be treated as intermediates in an overall two-electron transfer process eventually leading to thermodynamically stable products in the stable oxidation states Pt^{IV} and Tl^{I}.[9,10]

Another indication of the changed oxidation states of the metals in these compounds is provided by the bond lengths Tl−O and Tl−N. The bond lengths Tl−O (average 2.295 Å) in **1** and Tl−N (average 2.376 Å) in **3** are somewhat longer than those in $[Tl(DMSO)_6]^{3+}$ [2.227(3) Å][23] and $[Tl(en)_3]^{3+}$ (average 2.370 Å).[16] The slight increase of the bond lengths, despite the lower coordination number in the studied Pt−Tl compounds, is compatible with the change of the oxidation states of the metal ions upon formation of the Pt−Tl bond.

A detailed discussion of the oxidation states of the metal ions is outside the scope of the present work and will be discussed in a forthcoming paper.

Spin-Spin Coupling Constants

The very large values of the spin-spin coupling constants are the most striking feature of the bimetallic Pt−Tl complexes. For the en complexes, they are of the same order as for the Pt−Tl complexes with cyanide (cf. Table 1).[10] It is clear that all the spin-spin coupling constants (except $Pt-C^{C}$) decrease upon coordination of additional ligands L (L = cyanide, bipyridine and ethylenediamine) to the thallium side of the metal−metal entity $[(NC)_5Pt-TlL_n]$. The probable origin for the large coupling constants is the fact that the relativistic contraction of the 6s shell of thallium leads to an increase of 6s electron density on the Tl nucleus. This in turn contributes to the dominant Fermi contact term for the spin-spin coupling which is reflected in large values of $J(^{205}Tl-X)$. A similar situation occurs in the species Hg_3^{2+} where the enormous isotropic spin-spin coupling constant, $^{1}J(^{199}Hg-^{199}Hg)$ = 139600 Hz, is due to the large 6s contribution to the Hg−Hg bond and the large 6s electron density at the mercury nucleus caused by relativistic effects on this heavy atom.[33]

Conclusions

A new series of small Pt−Tl bonded clusters $[(NC)_5Pt-Tl(en)_{n-1}]$ (n = 1−3, for **1**, **2** and **3** respectively) was obtained in DMSO solution from reactions between $[Pt(CN)_4]^{2-}$, $[Tl(en)_n]^{3+}$ (n = 1, 3) and CN^-. The existence of a metal−metal bond in the three complexes was proved in solution by multinuclear NMR spectroscopy [spin-spin coupling constants $^{1}J(^{205}Tl-^{195}Pt)$ in the range 48000−66000 Hz], and in the solid by single crystal X-ray diffraction [Pt−Tl bond length = 2.6131(4) and 2.6348(5) Å, in the solid compounds **1** and **3,** respectively]. Additional support for the Pt−Tl bond was obtained from the metal−metal vibration in the FT Raman spectra of the solids. These solids comprise the shortest Pt−Tl metal−metal bonds among the hitherto structurally known solid compounds[1−8] and constitute the first single crystal structure information of the growing family of "naked" Pt−Tl bond clusters.

The new family of metal−metal bonded, photosensitive compounds synthesized during the last few years, $[(NC)_5Pt-Tl(CN)_{n-1}]^{(1-n)}$ (n = 2−4), has now been enlarged by three new members containing a nitrogen-coordinated thallium (Figure 6). If, as suggested previously,[9,10] these metal−metal bonded compounds are to be used in photovoltaic solar cells,[12] or to serve as a model for such a photovoltaic system, then their structure should be tuned to have properties appropriate for this type of cell, e.g. light absorption in a large part of the visible spectrum, reversible light-induced electron transfer, suitable redox potential and ion diffusion properties in solution. The presently studied Pt−Tl compounds with ethylenediamine can be seen in this

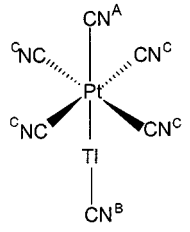

Figure 6. Sketch of the Pt−Tl compound **II** showing the notation for the cyanide sites

context as a first modification showing that tuning of the properties by means of nitrogen coordinating ligands is feasible.

Experimental Section

The solid compounds thallium(III) trifluoroacetate [Aldrich, $Tl(CF_3CO_2)_3$], potassium tetracyanoplatinate(II) [Aldrich, $K_2Pt(CN)_4$], sodium cyanide (Merck, Germany, NaCN), platinum(II) chloride (Aldrich, $PtCl_2$, 98%), sodium cyanide-^{13}C (Cambridge Isotope Laboratories, $Na^{13}CN$, ^{13}C 99%), thallium(I) carbonate (Aldrich, Tl_2CO_3, 99.95%) and liquid ethylenediamine (Merck, 99%) were all analytical grade and were used without further purification. DMSO was dried over molecular sieves (4 Å). During all experimental work the Pt−Tl compounds were protected from light.

$Tl(ClO_4)_3$ Stock Solution: Solid $TlClO_4$ was prepared from Tl_2CO_3 and an equivalent amount of $HClO_4$ and recrystallized from water. An acidic stock solution of $Tl(ClO_4)_3$ (1.2 M) was prepared by anodic oxidation of $TlClO_4$.[34a][34b] The Tl^{III} and acid concentrations were determined by titration with 0.1 M standard NaOH and $KBrO_3$ solutions after adding an excess of solid NaCl to the analyzed solution and using methyl orange as indicator.[34c]

Solid $[Tl(en)_3](ClO_4)_3$: Liquid ethylenediamine (0.08 mL, 1 mmol) was dissolved in 2 mL water. Then, a portion of the acidic aqueous solution of $Tl(ClO_4)_3$ (1.2 M; 0.21 mL 0.25 mmol) was added slowly under stirring. A black precipitate formed instantaneously, but dissolved soon thereafter. After addition of all the thallium (en/Tl ratio 3:1) the solution turned black again. Then, an approximate 10-fold excess of ethylenediamine was added and after half an hour of stirring the solution became colorless. The solution (at pH ≈ 10) was kept in a refrigerator; white round crystals formed at the bottom of the flask. The solution was filtered off and the crystals were dried in vacuum. The thallium content of the crystal compound $[Tl(en)_3](ClO_4)_3$ was determined by ICP (Inductively Coupled Plasma Atomic Emission Spectroscopy): calcd. 29.9%; found 30.1%.

The Raman spectra of $[Tl(en)_3](ClO_4)_3$ were recorded with a Renishaw System 1000 spectrometer equipped with a microscope (Leica DMLM). The band positions and assignment are as follows: 2976s, 2961s, 2897s (NH_2 and CH_2 str.); 1468m, 1278m (CH_2 and NH_2 bend); 1143m, 1021m (CN and CC str.); 936vs, 622s (ClO_4^- str.); 443vs, 302s (TlN str.). Abbreviations: vs: very strong; s: strong; m: medium.

Solid $[Tl(DMSO)_6](ClO_4)_3$: A portion of the acidic aqueous solution of $Tl(ClO_4)_3$ (1.2 M; 80 μL 0.1 mmol) was slowly added to freshly distilled DMSO (1 mL) under stirring. After addition of each drop of the concentrated $Tl(ClO_4)_3$ solution a white precipitate appeared but dissolved quickly. The colorless solution, kept in the dark, was degassed for 10 minutes with a water pump in a vacuum desiccator, and then degassed for 10 minutes again after three days. White cube-shaped crystals were obtained at the bottom of the flask. The composition of $[Tl(DMSO)_6](ClO_4)_3$ was proved by solving the crystal structure by single crystal X-ray diffraction and by Raman and infrared spectroscopic data.[23]

Preparation of Pt−Tl Compounds in Solution: For the synthesis of compound **1** (reaction 1) the solid compounds $[Tl(DMSO)_6](ClO_4)_3$ and $K_2Pt(CN)_4$ (0.05 mmol each) were dissolved in 1 mL DMSO. Then, a DMSO solution containing NaCN (0.05 mmol) was added.

Synthesis of compound **2** (reactions 2 and 3): $[Tl(en)](CF_3COO)_3$ was prepared in 1 mL DMSO by mixing $Tl(CF_3COO)_3$ (0.05 mmol) and liquid en (0.06 mmol). Then, solid $K_2Pt(CN)_4$ (0.05 mmol) was added, followed by addition of a DMSO solution containing NaCN (0.05 mmol).

Compound **3** (reaction 4): Crystalline powder samples of $[Tl(en)_3](ClO_4)_3$ and $K_2Pt(CN)_4$ (0.05 mmol each) were dissolved in 1 mL DMSO. Then, NaCN (0.05 mmol) in DMSO solution was added slowly with stirring. The reaction was slow; after two/three days a high concentration of the product was achieved. For the synthesis of ^{13}C enriched compounds **1, 2** and **3**, totally enriched compounds $Na_2Pt(^{13}CN)_4$ and $Na^{13}CN$(s) were used. $Na_2Pt(^{13}CN)_4$ was prepared in DMSO solution by the reaction between $PtCl_2$(s) and $Na^{13}CN$(s) in 1:4 molar ratio.

Preparation of Crystals: Crystals suitable for Raman and X-ray diffraction experiments were crystallized from solutions used in the NMR measurements. **1·(DMSO)**: 1 mL DMSO solution containing 0.05 mmol $[Tl(DMSO)_6](ClO_4)_3$, $K_2Pt(CN)_4$ and NaCN in a 1:1:1 molar ratio was kept in a vacuum desiccator in the dark. White small round crystals formed at the bottom of the flask after several days. **3·(2DMSO)**: A DMSO solution containing $[(NC)_5Pt-Tl(en)_2]$ (as proved by ^{205}Tl NMRspectroscopy) was degassed for 10 minutes with a water pump in a vacuum desiccator, and after three days degassed again for 10 minutes. After slow evaporation of DMSO under vacuum, rod-shaped white crystals appeared after several days. The crystals used for X-ray structural analysis were collected by filtration and recrystallized from DMSO using the same procedure as described above. Raman spectra of the solid compounds **1** and **3** were recorded with a Renishaw System 1000 spectrometer equipped with a microscope (Leica DMLM). The band positions and assignments are as follows: **1:** 3003m, 2919s (CH_3 str.); 2184s ($C{\equiv}N^A$ str.); 2174m, 2161m ($C{\equiv}N^C$ str.), 1419m, 1318w, 986m, 923m (CH_3 bend), 720s, 684s (CS str.), 453s (TlO str.), 389m, 334m (CSC or OSC bend), 154vs (Pt−Tl str.). **3:** 2950m, 2917s, 2889m (NH_2 and CH_2 str.), 2179s ($C{\equiv}N^A$ str.), 2168m, 2151m ($C{\equiv}N^C$ str.), 1452w, 1416w (CH_2 and NH_2 bend), 1094w, 1012m (CN and CC str.), 430s, 366s (TlN str.), 156vs (Pt−Tl str.). Abbreviations: vs: very strong; s: strong; m: medium; w: weak.

NMR Measurements: All NMR measurements were performed with a Bruker DMX500 spectrometer at a probe temperature of 25 ± 0.5 °C. DMSO was used as solvent for ^{205}Tl and ^{195}Pt NMR measurements and [D$_6$]DMSO for ^{13}C and ^1H NMR spectra.

^{205}Tl NMR spectra were recorded at SF = 288.49 MHz; typical NMR parameters: flip angle ≈30°; spectral window = 86 kHz; pulse repetition time = 0.5 s for Tl^{III} and 1s for Tl^I. The chemical shifts are reported in ppm toward higher frequency with respect to an external aqueous solution of $TlClO_4$ extrapolated to infinite dilution.

^{195}Pt NMR spectra were recorded at SF = 107.49 MHz with typical NMR parameters: flip angle ≈45°; spectral window = 91.4 kHz, pulse repetition time 2.5 s. The chemical shifts are given in ppm toward higher frequency from $\chi(^{195}Pt)$ = 21.4 MHz; $\delta[PtCl_6]^{2-}$ = 4533 at 25 °C in aqueous solution.

^{13}C NMR spectra were recorded at SF = 125.7 MHz with typical NMR parameters: flip angle ≈30°; spectral window = 25.1 kHz; pulse repetition time = 1.5 s; proton decoupled. The chemical shifts are reported in ppm with respect to the DMSO signal at δ = 39.5 from TMS.

^1H NMR spectra were recorded at SF = 500.1 MHz; flip angle ≈ 30°; pulse repetition time = 2 s. Chemical shifts are given in ppm with respect to the DMSO signal δ = 2.49 from TMS.

X-ray Crystal Structure Determination

Data Collection and Refinement: Suitable crystals of **1·(DMSO)** and **3·(2DMSO)** were selected under a polarizing microscope and mounted on a glass fiber. The data were collected on a Stoe image-plate diffractometer and were corrected for Lorentz, polarization and absorption effects using the X-SHAPE program package.[35] The structures were solved by direct methods (SHELXS-97)[36] and refined by full matrix least-squares on F^2 (SHELXL-97).[37] All non-hydrogen atoms were refined anisotropically. Hydrogen atoms were added at their ideal positions and refined using a riding model. Compound **3·(2DMSO)** was refined as a racemic twin [Flack parameter = 0.436(14)] since refinement in the centrosymmetric space group $P2_1/m$ introduced severe disorder in the DMSO molecules and unrealistically short C−C bonds in the en groups. In molecule **1**, the S4 atom of the DMSO ligand was treated as being disordered with occupancy factors of 0.78(1) and 0.22(1) for S4 and S4a, respectively. Selected crystal data for compound **1** and **3** are listed in Table 4.

Table 4. Selected crystal data for $[(NC)_5Pt-Tl(DMSO)_4]$-(DMSO)(**1**) and $[(NC)_5Pt-Tl(en)_2](DMSO)_2$ (**3**)

	1	**3**
Empirical formula	$C_{15}H_{30}N_5O_5PtS_5Tl$	$C_{13}H_{20}N_9O_2PtS_2Tl$
Mw	920.25	797.95
Crystal system	Monoclinic	Monoclinic
Space group	*Cc* (No. 9)	$P2_1$ (No. 4)
a, Å	17.2367(14)	9.3167(14)
b, Å	9.5560(11)	12.3007(13)
c, Å	17.7941(15)	11.4586(16)
β (deg)	100.551(10)°	112.318(16)°
V, Å^3	2881.4(5)	1214.8(3)
Z	4	2
Crystal size (mm^3)	0.14 × 0.28 × 0.30	0.12 × 0.12 × 0.30
ρ_{calc}, g cm^{-3}	2.1214(1)	2.1650(5)
Temperature, K	110(1)	110(1)
μ (Mo-K_α) (mm^{-1})	10.83	12.57
F(000)	1736.0	724.0
N(obs), *N*(par)	4785, 299	3526, 259
R(int)[a]	0.0360	0.0278
Flack parameter	0.000(6)	0.436(14)
S (goodness of fit)	1.140	1.032
*R*1, *wR*2 [$I > 2\sigma(I)$]	0.0197, 0.0485	0.0236, 0.0532
$\Delta\rho_{max}$, $\Delta\rho_{min}$ (e/Å^3)	1.103, −1.331	1.156, −0.944

[a] R values are defined as: $R(\text{int}) = \Sigma|F_o^2 - F_o^2(\text{mean})|/\Sigma[F_o^2]$, $S = [\Sigma[w(F_o^2 - F_c^2)^2]/(n-p)]^{1/2}$
$R1 = \Sigma||F_o| - |F_c||/\Sigma|F_o|$
$wR2 = [\Sigma[w(F_o^2 - F_c^2)^2] / \Sigma[w(F_o^2)^2]]^{1/2}$

Supporting Information Available

^{205}Tl and ^{195}Pt NMR spectra for compounds 1 and 2 are given in the Supporting Information. Ordering information is given on any current masthead page.

Crystallographic data (excluding structure factors) for the structures reported in this paper have been deposited with the Cambridge Crystallographic Data Centre as supplementary publications no. CCDC-145994 (**1**) and -145993 (**3**). Copies of the data can be obtained free of charge on application to CCDC, 12 Union Road, Cambridge CB2 1EZ, UK [Fax: (internat.) +44-1223/336-033; E-mail: deposit@ccdc.cam.ac.uk].

Acknowledgments

The continuous financial support of the Swedish Natural Science Research Council (NFR) is gratefully acknowledged. The authors thank European Commission's INTAS program and the Carl Trygger Foundation for financial support, and the Swedish Institute for the fellowship for G.-B. Ma′s stay in Stockholm.

[1] J. K. Nagle, A. L. Balch, M. M. Olmstead, *J. Am. Chem. Soc.* **1988**, *110*, 319−321.
[2] A. Balch, S. Rowley, *J. Am. Chem. Soc.* **1990**, *112*, 6139.
[3] O. Renn, B. Lippert, *Inorg. Chim. Acta* **1993**, *208*, 219−223.
[4] R. Uson, J. Fornies, M. Tomas, R. Garde, P. Alonso, *J. Am. Chem. Soc.* **1995**, *117*, 1837−38.
[5] O. Ezomo, M. P. Mingos, I. D. Williams, *J. Chem. Soc., Chem. Commun.* **1987**, 924−925.
[6] L.-J. Hao, J. J. Vittal, R. J. Puddephatt, *Inorg. Chem.* **1996**, *35*, 269−270.
[7] L.-J. Hao, J. Xiao, J. J. Vittal, R. J. Puddephatt, L. Manojlovic-Muir, K. W. Muir, A. A. Torabi, *Inorg. Chem.* **1996**, *35*, 658−666.
[8] L.-J. Hao, J. J. Vittal, R. J. Puddephatt, *Organometallics* **1996**, *15*, 3115.
[9] K. E. Berg, J. Glaser, M. C. Read, I. Tóth, *J. Am. Chem. Soc.* **1995**, *117*,7550.
[10] M. Maliarik, K. Berg, J. Glaser, M. Sandström, I. Tóth, *Inorg. Chem.* **1998**, *37*, 2910.
[11] M. Maliarik, J. Glaser, I. Tóth, M. W. da Silva, L. Zekany, *Eur. J. Inorg. Chem.* **1998**, 565.
[12] Md. K. Nazeeruddin, P. Liska, J. Moser, N. Vlachopoulos, M. Grätzel, *Helv. Chim. Acta* **1990**, *73*, 1788.
[13] M. G. B. Drew, O. W. Howarth, N. Martin, G. G. Morgan, J. Nelson, *J. Chem. Soc., Dalton Trans.* **2000**, 1275−1278.
[14] S. Musso, PhD thesis, ETH-Zurich, Switzerland, **1993**.
[15] J. Blixt, J. Glaser, P. Solymosi, I. Tóth, *Inorg. Chem.* **1992**, *31*, 5288−97.
[16] G.-B. Ma, A. Ilyukhin, J. Glaser, I. Tóth, L. Zekany, submitted.
[17] K. Nakamoto, *Infrared and Raman spectra of Inorganic and Coordination Compounds*, 4th ed., John Wiley & Sons, New York, **1986**, p 536.
[18] D. F. Shriver, C. B. Copper, in *Advances in Infrared and Raman spectroscopy* (Eds.: R. J. H. Clark, R. E. Hester), Heyden, London, **1980**, Vol. 6, pp 127−157.
[19] M. N. Memering, L. H. Jones, J. C. Bailar, *Inorg. Chem.* **1973**, *12*, 2793.
[20] G.-B. Ma, M. Kritikos, M. Maliarik, J. Glaser, submitted.
[21] J. Farideh, PhD Thesis. The Royal Institute of Technology (KTH), Stockholm, **2000**, p160.
[22] B. D. James, M. B., Millikan, M. F., Mackay, *Inorg. Chim. Acta* **1983**, *77*, L251.
[23] G.-B. Ma, A. Molla-Abbassi, A. Ilyukhin, V. Kessler, M. Skripkin, M. Kritikos, M. Sandström, J. Glaser, J. Näslund, I. Persson, submitted.
[24] [24a] R. J. Kostelnik, A. A. Bothner-By, *J. Magn. Reson.* **1974**, *14*, 141−151. − [24b] R. A. Haberkorn, L. Que, W. O. Gillum, R. H. Holm, C. S. Liu, R. C. Lord, *Inorg. Chem.* **1976**, *15*, 2408−2414.
[25] L. C. Damude, P. A. W. Dean, *J. Organomet. Chem.* **1979**, *168*, 123−138.
[26] I. M. Armitage, R. T. Pajer, A. J. M. Schoot Uiterkamp, J. F. Chlebouski, J. E. Coleman, *J. Am. Chem. Soc.* **1976**, *98*, 5710−5712.
[27] B. Birgersson, R. E. Carter, T. Drakenberg, *J. Magn. Reson.* **1977**, *28*, 299−302.
[28] A. D. Bain, D. R. Eaton, R. A. Hux, J. P. K. Tong, *Carbohydr. Rev.* **1980**, *84*, 1−12.
[29] H. J. Jakobsen, P. D. Ellis, *J. Phys. Chem.* **1981**, *85*, 3367−3369.
[30] [30a] N. F. Ramsey, *Phys. Rev.* **1950**, *78*, 699. − [30b] J. Mason, *Chem. Rev.* **1987**, *87*, 1299.
[31] H. Nakatsuji, K. Kanda, K. Endo, T. Yonezawa, *J. Am. Chem. Soc.* **1984**, *106*, 4653−4660.
[32] [32a] J. Blixt, B. Györi, J. Glaser, *J. Am. Chem. Soc.* **1989**, *111*, 7784. − [32b] P. Laszlo, *NMR of Newly Accessible Nuclei*, Vol. 2; Academic Press: New York, **1983**. − [32c] J. Mason, *Multinuclear NMR*, Plenum Press: New York, **1987**.
[33] R. J. Gillespie, P. Granger, K. R. Morgan, G. J. Schrobilgen, *Inorg. Chem.* **1984**, *23*, 887−891.
[34] [34a] G. Biedermann, *Arkiv. Kemi* **1953**, *5*, 441. − [34b] J. Glaser,

PhD Thesis. The Royal Institute of Technology (KTH), Stockholm, **1981**, p 15. − [34c] A. A. Noyes, J. L. Hoard, K. S. Pitzer, *J. Am. Chem. Soc.* **1935**, *57*, 1231.
[35] STOE, X-SHAPE revision 1.09, Crystal Optimisation For Numerical Absorption Correction, Darmstadt, Germany, **1997**.
[36] G. M. Sheldrick, *Acta Crystallogr.* **1990**, *A46*, 467−473.
[37] G. M. Sheldrick, SHELXL-97 Program for Refinement of Crystal Structures, University of Göttingen, Germany, **1997**.
Received October 4, 2000
[I00372]